A Service-Oriented Architecture for Body Area NanoNetworks with Neuron-based Molecular Communication

Article *in* Mobile Networks and Applications · December 2014

DOI: 10.1007/s11036-014-0549-0

5 authors, including:

Junichi Suzuki
University of Massachusetts Boston
166 PUBLICATIONS **2,064** CITATIONS

SEE PROFILE

Sasitharan Balasubramaniam
University of Nebraska at Lincoln
195 PUBLICATIONS **3,553** CITATIONS

SEE PROFILE

Sophie Pautot
SYNAXYS
34 PUBLICATIONS **1,409** CITATIONS

SEE PROFILE

Yevgeni Koucheryavy
Tampere University
432 PUBLICATIONS **7,886** CITATIONS

SEE PROFILE

Mobile Networks and Applications manuscript No.
(will be inserted by the editor)

A Service-Oriented Architecture for Body Area NanoNetworks with Neuron-based Molecular Communication

Junichi Suzuki · Sasitharan Balasubramaniam · Sophie Pautot · Victor Didier Perez Meza · Yevgeni Koucheryavy

Received: date / Accepted: date

Abstract Molecular communication provides communication and networking capabilities for nanomachines such as biosensors and bio-actuators to form and enable Body Area NanoNetworks (BANNs). This paper considers neuron-based molecular communication, which utilizes natural neurons as a primary component to build BANNs, and proposes an end-to-end software architecture to manage and control neuron-based BANNs through a series of software services. Those services aid to realize end user applications in healthcare, such as biomedical and rehabilitation applications. In the proposed architecture, a neuron-based BANN consists of a set of nanomachines and a network of neurons that are artificially formed into a particular topology. This paper investigates two mechanisms in the proposed architecture: (1) an artificial assembly method to form neurons into specific three-dimensional topology patterns and (2) a communication protocol for neuronal signaling based on Time Division Multiple Access (TDMA), called Neuronal TDMA. The assembly method uses silica beads as growth surface and bead-bead contacts as geometrical constraints on neuronal connectivity. A web lab experiment verifies this method with neuronal hippocampal cells. Neuronal TDMA leverages an evolutionary multiobjective optimization algorithm (EMOA) to optimize the signaling schedules for nanomachines. Simulation results demonstrate that the Neuronal TDMA efficiently obtains quality solutions.

Keywords Intrabody Nanonetworks · Molecular Communication · Neuronal signaling · Services · Evolutionary multiobjective optimization algorithms

This work is supported in part by the FiDiPro programme of Academy of Finland "Nanocommunication Networks" 2012–2016.

Junichi Suzuki
Department of Computer Science
University of Massachusetts, Boston, U.S.A.
Tel.: +1-617-287-6462
Fax: +1-617-287-6433
E-mail: jxs@cs.umb.edu
Present address: 100 Morrissey Blvd., Boston, MA 02125, USA

Sasitharan Balasubramaniam
Department of Electronics and Communication Engineering
Tampere University of Technology, Finland
E-mail: sasitharanb@gmail.com

Sophie Pautot
Center for Regenerative Therapies Dresden, Dresden, Germany
E-mail: sophie.pautot@crt-dresden.de

Victor Didier Perez Meza
Center for Regenerative Therapies Dresden, Dresden, Germany
E-mail: victor.perezmeza@crt-dresden.de

Yevgeni Koucheryavy
Department of Electronics and Communication Engineering
Tampere University of Technology, Finland
E-mail: yk@cs.tut.fi

1 Introduction

Nanoscale communication is a new research paradigm that aims to provide communication and networking capabilities between nanoscale devices (or nanomachines in short) such as biosensors and bio-actuators. Nanomachines are the most basic functional unit in nanoscale systems, and they perform very simple computation, sensing and/or actuation tasks [19].

One of a few nanoscale communication schemes is *molecular communication*, which is inspired by the communication mechanisms that occur among living cells. This bio-inspired communication scheme utilizes molecules as a communication medium [14]. Due to its properties such as inherent nanometer scale, biocompatibil-

ity and energy efficiency, a key application domain of molecular communication is Body Area NanoNetworks (BANNs) where nanomachines are networked to perform their tasks in the human body for biomedical and prosthetic purposes [1,4,14]. Those tasks include physiological sensing, biomedical anomaly detection, neural signal transduction and neuromuscular implant control.

This paper considers neuron-based molecular communication, which utilizes neurons as a primary component to build BANNs, and proposes an end-to-end software architecture to manage and control neuron-based BANNs through a series of software services. Those services may reside in clouds as well as the user's mobile devices (e.g., smartphones, tablets and laptops) and implantable devices/interfaces in order to connect low-level BANNs and higher-level end user applications such as biomedical and rehabilitation applications.

In the proposed architecture, a neuron-based BANN consists of a set of nanomachines and a network of neurons that are artificially formed into a particular topology. It allows nanomachines to interface (i.e., activate and deactivate) neurons in a non-invasive manner and communicate to other nanomachines through a chain of neurons with electrochemical signals. This paper investigates two mechanisms in the proposed architecture: (1) an artificial assembly method to form neurons into specific three-dimensional topology patterns and (2) a communication protocol for neuronal signaling based on Time Division Multiple Access (TDMA), called Neuronal TDMA. The assembly method uses silica beads as growth surface and bead-bead contacts as geometrical constraints on neuronal connectivity. A web lab experiment verifies this method with neuronal hippocampal cells and demonstrates it is feasible to realize communication substrates for neuron-based BANNs.

Neuronal TDMA performs a single-bit TDMA scheduling for nanomachines in neuron-based BANNs. It allows nanomachines to multiplex and parallelize neuronal signal transmissions while avoiding signal interference to ensure that signals reach the destination. It makes decisions of signaling schedules (i.e., when to activate neurons to trigger signal transmissions) for nanomachines with an evolutionary multiobjective optimization algorithm (EMOA) that evolves a set of solution candidates (or *individuals*). Each individual represents a particular TDMA schedule for nanomachines with respect to time. Neuronal TDMA considers *conflicting* optimization objectives such as signaling yield, signaling fairness among nanomachines and signaling delay. For example, improving signaling yield can degrade signaling fairness. On the contrary, improving signaling delay can degrade signaling yield.

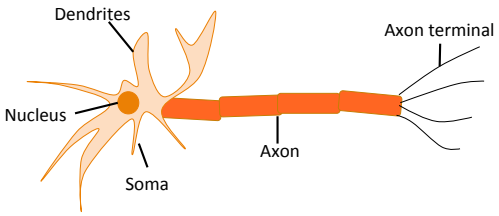

Fig. 1 The structure of neurons

Since there exists no single optimal solution (TDMA schedule) under conflicting objectives but rather a set of alternative solutions of equivalent quality, Neuronal TDMA is designed to seek the optimal trade-offs among the objectives by searching Pareto-optimal solutions that are equally distributed in the objective space. Therefore, it can produce both *extreme* TDMA schedules (e.g., the one yielding high signaling rate and low signaling fairness) and *balanced* schedules (e.g., the one yielding intermediate signaling delay and intermediate signaling rate) at the same time. Given a set of heuristically-approximated Pareto-optimal TDMA schedules, Neuronal TDMA allows BANN operators, software services and/or end users to examine the trade-offs among them and make a well-informed decision to choose one of them as the best TDMA schedule.

Simulation results show that Neuronal TDMA efficiently obtains quality solutions with acceptable computational costs and allows nanomachines to perform signal transmissions while avoiding signal interference. It outperforms several well-known existing EMOAs.

2 Background: Neurons and Neuronal Signaling

Neurons are a fundamental component of the nervous system, which includes the brain and the spinal cord. They are electrically excitable cells that process and transmit information via electrochemical signaling.

A neuron consists of cell body (soma), dendrites and axon (Fig. 1). The diameter of a soma varies from 4 to 100 micrometers. Dendrites are thin structures that arise from the soma. The length of a dendrite is up to a few hundred micrometers. An axon is a cellular extension that arises from the soma. It travels through the body in bundles called nerves. Its length can be over one meter in the human nerve that arises from the spinal cord to a toe.

Neurons are connected with each other via *synapses*, each of which is a junction between two neurons. A synapse contains molecular machinery that allows a (presynaptic) neuron to transmit a chemical signal to another (postsynaptic) neuron. Signals are transmitted from the axon of a presynaptic neuron to a dendrite of

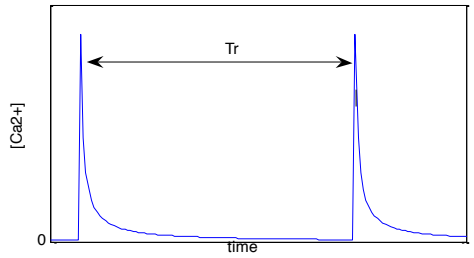

Fig. 2 Intercellular Ca^{2+} concentration in a neuron. Ca^{2+} releases must be separated by at least the refractory time T_r.

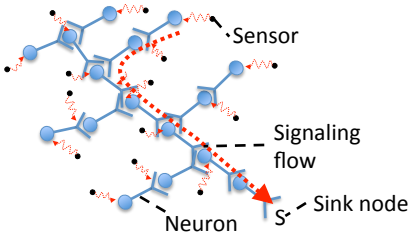

Fig. 3 An Example Neuron-based BANN

a postesynaptic neuron. An axon transmits an output signal to a postsynaptic neuron, and a dendrite receives an input signal from a presynaptic neuron.

Presynaptic and postsynaptic neurons maintain voltage gradients across their membranes by means of voltage-gated ion channels, which are embedded in the presynaptic membrane to unbalance intracellular and extracellular concentration of ions (e.g., Ca^{2+}) [18]. Changes in the cross-membrane ion concentration (i.e., voltage) can alter the function of ion channels. If the concentration changes by a large enough amount (e.g., approximately 80 mV in a giant squid), ion channels start pumping extracellular ions inward. Upon the increase in intracellular ion concentration, the presynaptic neuron releases a chemical called a *neurotransmitter* (e.g., acetylcholine), which travels through the synapse from the presynaptic postsynaptic neuron. The neurotransmitter electrically excites the postsynaptic neuron, which in turn generates an electrical pulse called an *action potential*. This signal travels rapidly along the neuron's axon and activates synaptic connections (i.e., opens ion channels) when it arrives at the axon's terminals. This way, an action potential triggers cascading neuron-to-neuron communication.

Fig. 2 shows how Ca^{2+} concentration changes in a neuron. When the concentration peaks, the neuron releases neurotransmitters and goes into a *refractory period* (T_r), in which the neuron replenishes its internal Ca^{2+} store. During T_r, it cannot receive and process incoming signals. The refractory period is approximately two milliseconds in a giant squid.

3 Related Work

Several types of solutions have been investigated for molecular communication, such as calcium signaling [15], bacteria communication [10] and molecular motors [13]. Most of these solutions are applicable to short-range communication (nanometers to millimeters), which often mimics wireless communication paradigms [5]. In contrast, this paper studies a long-range communication (millimeters to meters) that leverages wired neuronal networks. Neuron-based communication has such advantages as long distance coverage, high speed signaling (up to 90 m/s) and low attenuation in signaling [5].

Balasubramaniam et al. first examined TDMA communication for neuronal signaling [2]. This paper extends it with a multiobjective optimization algorithm that considers communication performance objectives such as signaling yield, fairness and latency. This paper also examines an artificial assembly method to form neurons into specific topology patterns.

Tezcan et al. address communication robustness in TDMA-based neuronal signaling by proposing a signal buffering mechanism with neural delay lines, which parallel fiber delay lines in optical network switching [20]. This paper is similar to their work in that both assume TDMA communication. However, this paper focuses on optimization in TDMA scheduling while Tezcan et al. do not consider TDMA scheduling.

4 A Service-Oriented Architecture for Neuron-based Body Area NanoNetworks

This section provides an overview of the proposed service-oriented architecture for neuron-based BANNs, in particular focusing on the use of artificial neuronal networks as physical molecular communication media.

The proposed architecture assumes neuronal signaling in a three-dimensional network of neurons that are artificially grown and formed into particular topology patterns. (This type of neuronal networks are often referred to as *artificial* neuronal networks in the rest of this paper.) In particular, the architecture assumes low-density neuronal networks [9].

Fig. 3 illustrates a schematic neuron-based BANN. It contains an artificial neuronal network and several nanomachines such as sensors and a sink. Sensors utilize neuronal signaling to deliver sensor data to the sink. As a potential application, sensors may periodically monitor certain physiological status and report

physiological data or biomedical anomalies to the sink. This paper assumes that nanomachines (e.g., sensors) interact with neuronal networks in a *non-invasive* manner. This means that it is not required to insert particular materials (e.g., carbon nanotubes) into neurons so that nanomachines can trigger and receive signals. For example, nanomachines may use chemical agents (e.g., acetylcholine and mecamylamine [2]) or light [7].

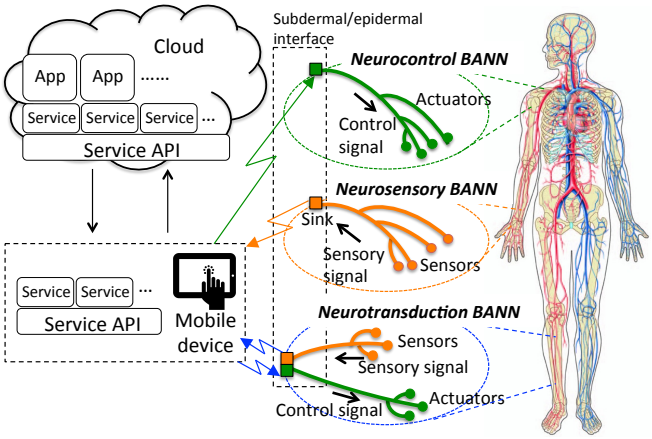

Fig. 4 An Overview of the Proposed Service-Oriented Architecture

The proposed architecture supports three types of neuron-based BANNs: (1) neurosensory BANNs, (2) neurocontrol BANNs and (3) Neurotransduction BANNs (Fig. 4). A neurosensory BANN has sensor nanomachines transmit sensory data to the sink nanomachine. (See Fig. 3 as an example of this BANN.) Example sensors include electrodes that are interfaced to a nerve for collecting and intercepting neuronal signals as well as biosensors to monitor physiological parameters and detect biomedical anomalies. The sink serves as a subdermal or epidermal interface that connect a neuron-based BANN with external devices by converting incoming electrochemical signals to electrostatic or electromagnetic signals. If electrostatic signals are used, they realize a body-coupled communication scheme [16,21] for carrying sensory data to an epidermal device(s) such as a smartphone that the user holds and a device that is embedded in the floor the user stands on. If electromagnetic signals are used, they realize radio frequency communications to carry sensory data to an around-body mobile device(s) such as a smartphone and tablet.

A neurocontrol BANN has a subdermal/epidermal interface node receive control signals from on/around-body mobile devices and fire its neighboring neuron to transmit the control signals to actuator nanomachines (Fig. 4). Example actuators include bio-actuators that

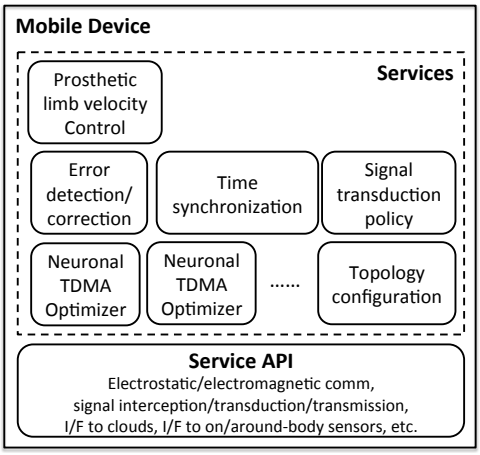

Fig. 5 Services and Service API in a Mobile Device

are equipped with pumps to release drug molecules as well as neurostimulators that are interfaced to a nerve in order to issue high/low-frequency stimulation to prevent/allow neuronal signaling in the nerve.

A neurotransduction BANN is a hybrid of a neurosensory BANN and a neurocontrol BANN. It has sensor nanomachines transmit sensory signals to a subdermal/epidermal interface node, which combines a sink nanomachine with a control signaling nanomachine (Fig. 4). The interface node transduces an incoming sensory signal to a control signal and fires its neighboring neuron to transmit the control signal to actuator nanomachines. The node may communicate with the user's mobile device.

Potential application of neurotransduction BANNs are neurointerfaces that leverage in-situ sensing and actuation for prosthetic devices. For example, a BANN may be used to connect a nerve arising from the spinal cord to a prosthetic device [12]. In this BANN, sensors intercept neuronal signals from a nerve and fire their neighboring neurons to transmits signals to a subdermal/epidermal node through an artificial neuronal network. The node in turn aggregates incoming signals and fires its neighboring neuron to transmit a signal to actuators through another neuronal network. Upon signal arrivals, the actuators control prosthetic devices accordingly. A neurotransduction BANN may also be used for the opposite interface direction: from a prosthetic device to neurons arising from the spinal cord [17]. In this BANN, sensors are interfaced to a prosthetic device and transmit signals to actuators such as neurostimulators through two artificial neuronal networks.

As shown in Fig. 4, the proposed architecture allows software services to be deployed on the user's mobile device and/or cloud computing platforms. Fig. 5 illustrates an organization of the service API and services

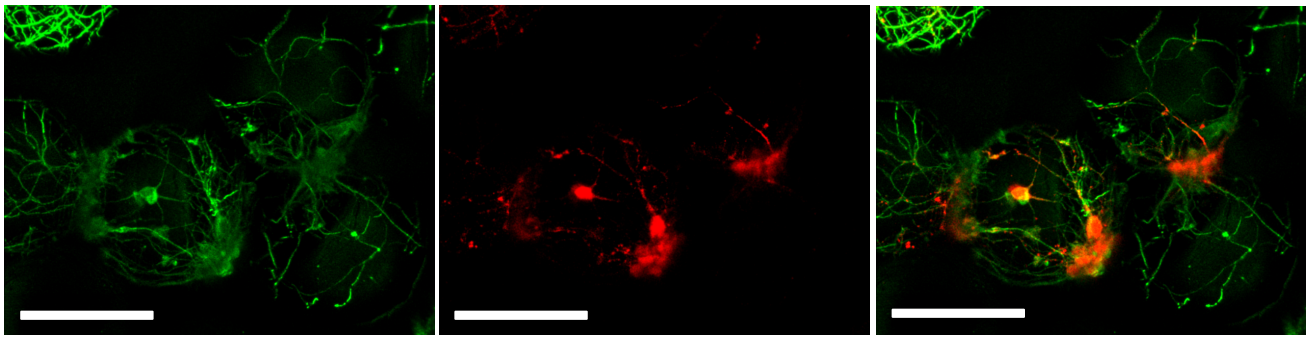

Fig. 6 After seven days in culture beads carrying E18 neuronal hippocampal cells were fixed and z-stack series were acquired with a laser scanning confocal microscope. The images are an XY projection of 100 mm confocal z series. Beads were held together by the neuronal processes growing over them. To trace all the neuronal processes the sample was stained with neuronal tubulin antibody (green) and to identify individual connections a small fraction of the neurons were treated to express a red marker (red).

in the user's mobile device. The service API provides foundational common functionalities to enable services on the mobile to interact with subdermal/epidermal interface nodes, on/around-body sensors and clouds. Individuals services are defined and used to control and manage neuron-based BANNs. For example, the topology configuration service maintains the topology of a neuronal network. Neuronal TDMA optimizers implement different EMOAs for TDMA scheduling.

Services are dynamically replaceable and reconfigurable. For example, Neuronal TDMA optimizers may be dynamically replaced to incorporate new TDMA scheduling requirements. The *prosthetic limb velocity control* service may be dynamically reconfigured to adjust the movement of a prosthetic limb. When the user walks in a dry environment, the control service may move the prosthetic limb at a regular velocity. However, as the user moves to an slippery (e.g., icy or wet) area, the service may be alerted and reconfigured to instruct the prosthetic limb to tread slowly. This alert may be manually generated by the user using his/her mobile device or automatically generated from devices embedded in the physical environment (e.g., the floor).

5 An Assembly of Artificial Neuronal Networks

The proposed neuron-based BANN architecture assumes three dimensional artificial neuronal networks. An example network is presented in Fig. 6. The method used to establish the topologically-specific neuronal network is by using 125 μm diameter silica beads as growth surface that are large enough for neuronal cell bodies and their processes. Monodisperse particles are chosen as they have the property to spontaneously assemble into an ordered array of connecting particles. The sites of bead-bead contact serve of crossing point for neuronal processes to extend onto neighboring beads, thus providing a geometrically determined constraint on connectivity. The bead surface was coated with poly-L-lysine (PLL) to enhance cell adhesion and to support neuronal maturation **13, 14**. Rat hippocampal neurons harvested at a late embryonic stage (E18) were seeded on PLL-coated beads following dissection and dissociation. The beads provided a growth surface for one to five neurons and allowed us to move them with minimum damaged to their processes. As neurons mature their processes decorate the particles. In order to trace processes from different cells, transfection of one bead culture is performed to express Tandem-Dimer-Tomato (TdT). After 48 hours in culture one bead culture carrying labeled is mixed with one bead culture carrying unlabeled neurons. To characterize the assemblies, confocal microscopy images of 450 μm x 450 μm x 388 μm subsections of the arrays were acquired. The maximum intensity Z-projection of xx plane show how processes decorate the bead surface, and allow us to distinguish processes and synapses between neurons. The cell tracing process was done manually.

6 Neuronal TDMA

When nanomachines invoke signaling on a neuronal network, they may transmit signals on the same neurons at the same time. This leads to a large number of interference (or collisions) in the neuronal network, which in turn leads to corruption of transmitted information at the sink nanomachine. As discussed in Section 2 and Fig. 2, neurons possess the refractory period in which no signals can be processed and transmitted. Thus, Neuronal TDMA is intended to eliminate signaling interference through a chain of neurons toward the sink by

scheduling which sensors activate which neurons with respect to time.

Neuronal TDMA is a single-bit TDMA communication protocol that periodically assigns a *time slot* dedicated to each sensor. Sensors activate neurons, one after the other, each using its own time slot. This allows multiple sensors to transmit signals to the sink through the shared neuronal network without interference. Each sensor transmits a single signal (a single bit) within a single time slot.

Fig. 7 shows an example neuron-based BANN that contains four nanomachines (three sensors and one sink) and a network of five neurons. Fig. 8 depicts an example TDMA schedule for those sensors to activate neurons. The scheduling cycle period lasts 6 time slots ($T_s = 6$). The input s_1 activates the neuron n_4 to initiate signaling in the first time slot T_1. The signal travels through n_5 in the next time slot T_2 to reach the sink. The input s_2 transmits a signal on n_3 in T_2. During T_2, two signals travel in the neuronal network in parallel. The duration of each time slot must be equal to, or longer than, the refractory period T_r (Fig. 2).

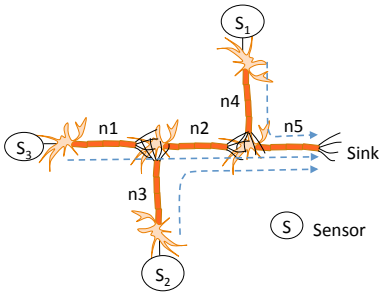

Fig. 7 An Example Neuron-based BANN

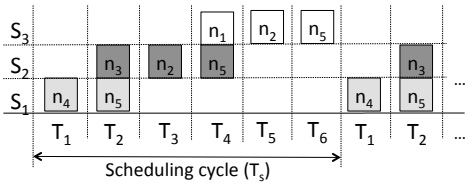

Fig. 8 An Example TDMA Schedule

The scheduling problem in Neuronal TDMA is defined as an optimization problem where a neuron-based IBSAN contains M sensors, $S = \{s_1, s_2, ..., s_i, ..., s_M\}$, and N neurons, $N = \{n_1, n_2, ..., n_j, ..., n_N\}$. Each sensor transmits at least one signals to the sink during the scheduling cycle T_s. $E^{s_i} = \{E_1^{s_i}, E_2^{s_i}, ...E_k^{s_i}, ..., E_{|E^{s_i}|}^{s_i}\}$ denotes the signals that a sensor s_i transmits to the sink. $|E^{s_i}|$ is the total number of signals that s_i transmits during the scheduling cycle T_s.

6.1 Optimization Objectives and Constraints

Neuronal TDMA considers three optimization objectives: (1) signaling yield, (2) signaling fairness among different sensors and (3) signaling delay.

Signaling yield (Y) is computed as follows. It is to be maximized.

$$f_Y = \sum_{i=1}^{M} |E^{s_i}| \tag{1}$$

This objective indicates the total number of signals that the sink receives from all M sensors during the scheduling cycle T_s.

The second objective, signaling fairness (F), is computed as follows. It is to be maximized.

$$f_F = \sum_{l=1}^{M} \sum_{m=1}^{M} \sum_{k=1}^{|E^{s_l}|} \frac{1}{|t_d^{k(s_l)} - t_d^{k(s_m)}|}, \quad l \neq m \tag{2}$$

$t_d^{k(s_l)}$ denotes the departure time of the k-th signal that s_l transmits to the sink. This objective encourages the sensors to equally access the shared neuronal network for signaling in order to avoid a situation where a limited number of sensors dominate the network. Higher fairness means that the sensors access the neuronal network more equally.

The third objective, signaling delay (D), is computed as follows. It is to be minimized.

$$f_D = max_{s_i \in S}\ t_a^{|E^{s_i}|((s_i)} \tag{3}$$

$t_a^{|E^{s_i}|((s_i)}$ denotes the arrival time at which the sink receives the last (the $|E^{s_i}|$-th) signal that s_i transmits. f_D indicates how soon the sink receives all signals from all M sensors. f_D determines the scheduling cycle period T_s ($T_s = f_D$).

Neuronal TDMA considers three constraints in its optimization process. The first constraint enforces that at most one signal can pass through each neuron in a single time slot. The second constraint enforces each sensor to transmit at least one signal to the sinks ($|E^{s_i}| \geq 1\ \forall i = 1, 2, ..., M$). The third constraint (C_D) is the upper limit for f_D: $f_D \leq C_D$. The delay constraint violation (g_D) is computed as follows where $I = 1$ if $f_D > C_D$ and $I = 0$ otherwise.

$$g_D = I \times (f_D - C_D) \tag{4}$$

6.2 Individual Representation

In Neuronal TDMA, each individual represents a particular TDMA schedule for M sensors. Fig. 9 shows the structure of an individual. In this example, the first sensor, s_1, activates the first neuron n_1 for signaling. The signal travels through two neurons, n_2 and n_3, in the second and third time slots t_2 and t_3, respectively.

S_3	0	0	1	0	0
S_2	0	1	0	0	0
S_1	1	0	0	0	0
	T_1	T_2	T_3	T_4	T_5

Fig. 9 Individual Representation

main
$t \leftarrow 0$
$P^0 \leftarrow$ Randomly generated μ_0 individuals
repeat
  $Q^0 \leftarrow \emptyset$
  repeat
    $p_1 \leftarrow$ BTounament(P^g)
    $p_2 \leftarrow$ BTounament(P^g)
    $q_c^1, q_c^2 \leftarrow$ Crossover(p_1, p_2)
    $q_m^1 \leftarrow$ Mutation(q_c^1)
    $q_m^2 \leftarrow$ Mutation(q_c^2)
    if $q_m^1 \notin Q^t$
      then $Q^t \leftarrow Q^t \cup q_m^1$
    if $q_m^2 \notin Q^t$
      then $Q^t \leftarrow Q^t \cup q_m^2$
  until $|Q^t| = \lambda_t$
  $P^{t+1} \leftarrow$ DiversityAwareSelection($P^t \cup Q^t$)
  $\lambda_{t+1} \leftarrow$ OffspringSizeAdjustment()
  $t \leftarrow t + 1$
until $t = t_{max}$

Fig. 10 Algorithmic Structure of the Proposed EMOA in Neuronal TDMA

6.3 The Proposed EMOA in Neuronal TDMA

Fig. 10 shows the algorithmic structure of the proposed EMOA in Neuronal TDMA. In the first generation ($t = 0$), μ individuals are randomly generated as the initial generation P^0. This process makes sure that generated individuals never violate constraints except the delay constraint C_D. In each generation (t), a pair of individuals, called parents (p_1 and p_2), are chosen from the current population P^g using the binary tournament operator (`BTounament()`) [6]. A binary tournament randomly takes two individuals from P^t, compares them based on their fitness values, and chooses a superior one (i.e., the one whose fitness is higher) as a parent.

The notion of fitness is defined with *constrained dominance relationships* among individuals. The relationships rank individuals based on the objective values and delay constraint violation that they yield. An individual i is said to *constrained-dominate* an individual j if:

- i does not violate the signaling delay constraint ($gD(i) = 0$; c.f. Equation 4) but j does ($gD(j) > 0$),
- both i and j do not violate the delay constraint, and i dominates j with respect to objectives, or
- both i and j violate the delay constraint, and the constraint violation of i is less than j's ($gD(i) < gD(j)$).

Given the notion of *dominance* [3], individual i is said to *dominate* individual j (denoted by $i \succ j$) with respect to objectives if:

- $f_k(i) \leq f_k(j)$ for all $k = 1, 2, ..., m$, and
- $f_k(i) < f_k(j)$ for at least one $k \in 1, 2, ...m$

$f_k(i)$ denotes the objective value that i yields in the k-th objective. For f_Y and f_F, their inverses are used here for an individual-to-individual comparison purpose because the two objectives are to be maximized.

Fitness is calculated for each individual (i) as follows.

$$Fitness(i) = \mu - d_i \tag{5}$$

μ denotes the population size, and d_i denotes the number of individuals that constrained-dominate i. Fitness proportionate the superiority of an individual.

After two parents (p_1 and p_2) are selected, they reproduce two offspring (q_c^1 and q_c^2) with a single-point crossover operator (`Crossover()` in Fig. 10). Each offspring is mutated with a mutation operator (`Mutation()` in Fig. 10) that randomly alters the time slot assignment for each neuronal signal at the mutation rate P_m. `Crossover()` and `Mutation()` make sure that offspring never violate constraints except the delay constraint C_D.

Once λ offspring are reproduced through parent selection, crossover and mutation, the proposed EMOA ranks $\mu + \lambda$ (i.e., $|P^t \cup Q^t|$) individuals and selects the top μ of them as the individuals used in the next generation (P^{t+1}) with a diversity-aware selection operator (`DiversityAwareSelection()` in Fig. 10). This operator ranks individuals based on their diversity in the objective space as well as their fitness values. It computes each individual's diversity with the notion of crowding distance [3]. A crowding distance indicates how an individual is distant from its nearest neighbors in the objective space. Thus, an individual with a higher crowding

distance exists in a less crowded region in the objective space. The proposed diversity-aware selection operator plots individuals in a two dimensional space whose axes represent their fitness and diversity. Then, it determines the dominance relationships among individuals with respect to the two axes and ranks them from the ones with higher fitness and diversity to the ones with lower fitness and diversity. Finally, it selects the top μ individuals as the next generation's individuals. The proposed diversity-aware selection operator is designed to maintain the diversity of individuals in order to reveal the trade-offs among conflicting objectives.

At the end of each generation (t), the proposed EMOA adjusts the number of offspring reproduced in the next generation (λ_{t+1}) (`OffspringSizeAdjustment()` in Fig. 10). λ_{t+1} is re-computed on a generation-by-generation basis in order to adjust the density of individuals in the objective space as well as the selection pressure of individuals. In this paper, selection pressure (ψ) is measured as follows:

$$\psi = \frac{\mu + \lambda}{\mu} \tag{6}$$

μ denotes the population size. Selection pressure indicates how hard individuals can survive to the next generation; a higher selection pressure means that individuals have lower chances to survive to the next generation. It is known that a low selection pressure significantly degrades optimization/convergence speed [6]. The proposed offspring size adjustment operator is designed to maintain a reasonably high selection pressure by adjusting λ in Equation 6.

The density of individuals in the objective space (η) is measured as follows:

$$\eta = \frac{\mu + \lambda}{\gamma} \tag{7}$$

γ denotes the total volume of the objective space. In a higher-dimensional objective space, it is harder to determine dominance relationships among individuals because individuals have higher chances to be non-dominated with each other [8]. This often leads to premature convergence, which fails to improve the quality of individuals. The proposed offspring size adjustment operator is designed to alleviate this problem by increasing λ in Equation 7 and in turn maintaining the density of individuals in the objective space.

The size of offspring is adjusted based on those in the current (the t-th) and previous (the $(t-1)$-th):

$$\lambda_{t+1} = \lambda_t + \left(\frac{\lambda'_{t-1}}{\lambda_{t-1}} - \frac{\lambda'_t}{\lambda_t} \right) \lambda_t \tag{8}$$

λ'_t denotes the number of offspring that survive to the next generation through the selection process in `DiversityAwareSelection()` (Fig. 10). Thus, $\frac{\lambda'_t}{\lambda_t}$ indicates the survival ratio of offspring. If is is lower than the survival ratio at the previous generation ($\frac{\lambda'_{t-1}}{\lambda_{t-1}}$), the proposed operator considers that convergence/evolution does not proceed well due to a lack of enough selection pressure and/or individual density in the objective space. Therefore, the operator increases the number of offspring reproduced in the next generation (λ_{t+1}). Conversely, if $\frac{\lambda'_t}{\lambda_t} > \frac{\lambda'_{t-1}}{\lambda_{t-1}}$, the operator decreases λ_{t+1}.

7 Simulation Evaluation

This section evaluates the proposed EMOA in Neuronal TDMA through simulations.

7.1 Simulation Configurations

This paper simulates a neuronal network that contains 43 neurons (Fig. 11). 11 sensors are evenly distributed in the network. Although a number of studies have investigated the topology shapes of neuronal networks, Diffusion Limited Aggregation (DLA) is a common method to represent and generate their tree topology shapes [11]. This paper uses a similar random tree-like topology that mimics a dendritic tree among neurons [11] (Fig. 11).

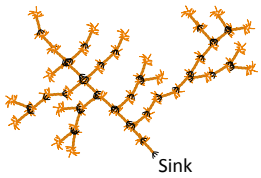

Fig. 11 A Simulated Neuronal Network

The proposed EMOA is configured with a set of parameters shown in Table 1. It is compared with two well-known existing EMOAs: NSGA-II [3] and SPEA2 [22]. Each experimental result is obtained from 20 independent experiments.

Table 1 EMOA Configurations

Parameter	Value
The initial population size (μ_0 in Fig. 10)	100
The initial offspring size λ_0 (μ_0 in Fig. 10)	100
Mutation rate (P_m in Fig. 10)	10%
The max. number of generations (g_{max} in Fig. 10)	100

7.2 Simulation Results

Fig. 12 shows how individuals increase the union of the hypervolumes that they constrained-dominate in the objective space as the number of generations grows in the proposed EMOA, NSGA-II and SPEA2. The hypervolume metric quantifies the optimality and diversity of individuals [23]. A higher hypervolume means that individuals are closer to the Pareto-optimal front and more diverse in the objective space. As Fig. 12 shows, the proposed EMOA rapidly increases its hypervolume measure in the first 10 generations and converges around the 60th generation. At the last generation, all individuals are non-constrained-dominated in the population. This verifies that the proposed EMOA allows individuals to efficiently evolve and improve their quality and diversity within 100 generation.

Fig. 12 also compares evolutionary convergence among the proposed EMOA, NSGA-II and SPEA2. All the three EMOAs initially increase hypervolume measures at a similar rate; however, the proposed EMOA converges to a higher hypervolume measure than NSGA-II and SPEA2. Fig. 12 shows that the proposed EMOA outperforms NSGA-II and SPEA2 in the quality and diversity of individuals.

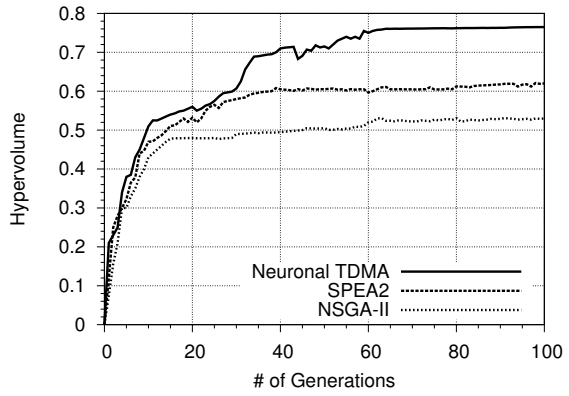

Fig. 12 Hypervolume

Table 2 compares the proposed EMOA, NSGA-II and SPEA2 with the coverage metric ($\mathcal{C}$-metric). This metric compares two sets of individuals [24]. Given individual sets A and B, $\mathcal{C}(A, B)$ measures the fraction of individuals in B that at least one individual in A dominates:

$$\mathcal{C}(A,B) = \frac{|\{b \in B \mid \exists a \in A : a \succ b\}|}{|B|} \tag{9}$$

The $\mathcal{C}$-metric values in Table 2 are computed with a set of individuals that each EMOA produces at the last generation. As shown in Table 2, $\mathcal{C}$(Neuronal TDMA, NSGA-II) is greater than $\mathcal{C}$(NSGA-II, Neuronal TDMA) ($0.55 > 0.0$). Also, $\mathcal{C}$(Neuronal TDMA, SPEA2) ¿ $\mathcal{C}$(SPEA2, Neuronal TDMA) ($0.45 > 0.0$). These results mean that the proposed EMOA outperforms NSGA-II and SPEA2 in the quality of individuals. No individuals of NSGA-II and SPEA2 can dominate the individuals of the proposed EMOA.

Table 2 C-metric Comparison

	$\mathcal{C}$-metric value
$\mathcal{C}$(Neuronal TDMA, NSGA-II)	0.55
$\mathcal{C}$(NSGAII, Neuronal TDMA)	0.0
$\mathcal{C}$(Neuronal TDMA, SPEA2)	0.45
$\mathcal{C}$(SPEA2, Neuronal TDMA)	0.0

Fig. 13 illustrates the diversity of individuals with the distribution metric This metric measures the degree of uniform distribution of individuals in the objective space. It is computed as the standard deviation of Euclidean distances among individuals:

$$\sqrt{\frac{\sum_{i=1}^{N-1}(d_i - \bar{d})^2}{N-1}} \tag{10}$$

d_i denotes the Euclidean distance between a given individual (the i-th individual in the population) and its closest neighbor in the objective space. $\bar{d}$ denotes the mean of d_i. N denotes the number of individuals in the population. The objective space is normalized to compute the distribution metric. Lower distribution means that individuals are more uniformly (or evenly) distributed.

As shown in Fig. 13, all three EMOAs improve the diversity of individuals as the number of generations grows. At the last generation, the proposed EMOA's distribution is less than the half of NSGAII's. Along with the evaluation with the hypervolume metric, the proposed EMOA outperforms NSGA-II and SPEA2 in the diversity of individuals.

Table 3 shows the average of each objective value. A value in parentheses indicates a standard deviation of objective values that an EMOA yields in 20 independent simulations. As this table illustrates, Neuronal TDMA yields the best objective values on average in all three objectives.

Table 3 Average Objective Values

	f_Y	f_F	f_D
Neuronal TDMA	22 (4.33)	0.10 (0.33)	22.86 (5.11)
NSGA-II	16.56 (3.09)	0.07 (0.99)	31.87 (7.33)
SPEA2	18.34 (3.96)	0.08 (0.10)	25.99 (6.44)

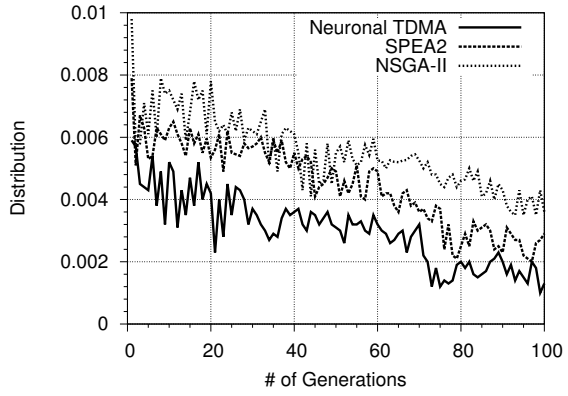

Fig. 13 Distribution

Table 4 shows how Neuronal TDMA yields three objective values, respectively, subject to different signaling delay constraints (C_D). Neuronal TDMA successfully meets both USD constraints. Given a more strict USD constraint ($C_D = 17$), it improves its f_D while degrading f_Y and f_F. Table 4 demonstrate that Neuronal TDMA can provide different optimization results under different constraints. This means that it allows Body Area NanoNetwork designers to examine various "what-if" analyses. For example, they can examine whether they can sacrifice f_Y by 35% and f_F by 50% to improve f_D by 25%. This way, Neuronal TDMA aids Body Area NanoNetwork designers to make well-informed scheduling decisions for signaling in Body Area NanoNetwork.

Table 4 Objective Values with Constraints

	f_Y	f_F	f_D
$C_D = 21$	18 (3.1)	6.1 (0.9)	20.17 (0.89)
$C_D = 17$	14 (2.5)	3.4 (0.4)	16.78 (1.01)

8 Conclusions

This paper considers neuron-based molecular communication, which utilizes natural neurons as a primary component to build BANNs, and proposes an end-to-end software architecture to manage and control neuron-based Body Area NanoNetworks (BANNs) through a series of software services. Those services aid to realize end user applications. This paper investigates two mechanisms in the proposed architecture: (1) an artificial assembly method to form neurons into specific three-dimensional topology patterns and (2) a communication protocol for neuronal signaling, called Neuronal TDMA. The assembly method uses silica beads as growth surface and bead-bead contacts as geometrical constraints on neuronal connectivity. A web lab experiment verifies this method with neuronal hippocampal cells. Neuronal TDMA leverages an evolutionary multiobjective optimization algorithm (EMOA) to optimize the signaling schedules for nanomachines. Simulation results demonstrate that the Neuronal TDMA efficiently obtains quality solutions.

Several extensions are planned over this work. First, an extended set of simulations is planned to investigate a neurotransduction BANNs (Fig. 4) while this paper's simulation study focuses on a neurosensory BANN. Another extension is to incorporate the notion of time synchronization among nanomachines in simulations. Moreover, the EMOA in Neuronal TDMA will be extended to handle noise in neuronal signaling and consider an extra objective, communication robustness, in addition to the current communication performance objectives (signaling yield, fairness and delay).

References

1. B. Atakan, S. Balasubramaniam, and O. B. Akan. Body area nanonetworks with molecular communications in nanomedicine. *IEEE Commun. Mag.*, 50(1):28 – 34, 2012.
2. S. Balasubramaniam, N. T. Boyle, A. Della-Chiesa, F. Walsh, A. Mardinoglu, D. Botvich, and A. Prina-Mello. Development of artificial neuronal networks for molecular communication. *Nano Commun. Netw.*, 2(2-3):150–160, 2011.
3. K. Deb, S. Agrawal, A. Pratab, and T. Meyarivan. A fast elitist non-dominated sorting genetic algorithm for multi-objective optimization: NSGA-II. In *Proc. Int'l Conference on Parallel Problem Solving from Nature*, 2000.
4. R. A. Freitas. Current status of nanomedicine and medical nanorobotics. *J. Comput. Theor. Nanosci.*, 2(1):1–25, 2005.
5. L. P. Gine and I. F. Akyildiz. Molecular communication options for long range nanonetworks. *Computer Networks*, 53:2753–2766, 2009.
6. D. E. Goldberg. *Genetic Algorithms in Search, Optimization and Machine Learning.* Addison Wesley, 1989.
7. C. Hosokawa, Y. Sakamoto, S. N. Kudoh, Y. Hosokawa, and T. Taguchi. Femtosecond laser-induced stimulation of a single neuron in a neuronal network. *Appl. Phys. A*, 110(3):607–612, 2013.
8. H. Ishibuchi, N. Tsukamoto, Y. Hitotsuyanagi, and Y. Nojima. Effectiveness of Scalability Improvement Attempts on the Performance of NSGA-II for Many-Objective Problems. In *Proc. ACM Conference on Genetic and Evol. Computat.*, 2008.
9. S. B. Jun, M. R. Hynd, N. Dowell-Mesfin, K. L. Smith, J. N. Turner, W. Shain, and S. J. Kima. Low-density neuronal networks cultured using patterned polyl-L-lysine on microelectrode arrays. *J. Neurosci. Methods*, 160(2):317–326, 2007.
10. P. Lio and S. Balasubramaniam. Opportunistic routing through conjugation in bacteria communication nanonetwork. *Nano Comm. Networks*, 3(1), 2012.

11. A. Luczak. Measuring neuronal branching patterns using model-based approach. *Front. Comput. Neurosci.*, 4(135), 2010.
12. M. R. Y. L. H. W. L. Moo Sung Chae, Zhi Yang. a 128-channel 6mw wireless neural recording ic with spike feature extraction and uwb transmitter. *IEEE Trans. Neur. Sys. Reh.*, 17(4):312 – 321, August 2009.
13. M. Moore, A. Enomoto, T. Nakano, R. Egashira, T. Suda, A. Kayasuga, H. Kojima, H. Sakakibara, and K. Oiwa. A design of a molecular communication system for nanomachines using molecular motors. In *Proc. IEEE Int'l Conference on Pervasive Computing and Communications Workshops*, 2006.
14. T. Nakano, M. Moore, F. Wei, A. V. Vasilakos, and J. W. Shuai. Molecular communication and networking: Opportunities and challenges. *IEEE Trans. Nanobiosci.*, 11(2):135–148, 2012.
15. T. Nakano, T. Suda, M. Moore, R. Egashira, A. Enomoto, and K. Arima. Molecular communication for nanomachines using intercellular calcium signaling. In *Proc. IEEE Int'l Conf. on Nanotechnology*, 2005.
16. K. Partridge, B. Dahlquist, A. Veiseh, A. Cain, A. Foreman, J. Goldberg, and G. Borriello. Empirical measurements of intrabody communication performance under varied physical configurations. In *Proc. User Interface Softw. Technol. Symposium*, 2001.
17. K. Y. Silvestro Micera, Xavier Navarro. Interfacing with the peripheral nervous system to develop innovative neuroprostheses. *IEEE Trans. Neur. Sys. Reh.*, 17(5):417 – 418, October 2009.
18. G. Stuart, J. Schiller, and B. Sakmann. Action potential initiation and propagation in rat neocortical pyramidal neurons. *Journal of Physiology*, 505.3, 1997.
19. T. Suda, M. Moore, T. Nakano, R. Egashira, and A. Enomoto. Exploratory research on molecular communication between nanomachines. In *Proc. ACM Genetic and Evol. Computat. Conference*, 2005.
20. H. Tezcan, S. Oktug, and F. N. Kok. Neural delay lines for tdma based molecular communication in neural networks. In *Proc. IEEE Int'l Conference on Communications*, 2012.
21. T. Zimmerman. Personal area networks (PAN): Near-field intra-body communication. *IBM Syst. J.*, 35(3-4):609–617, 1996.
22. E. Zitzler, M. Laumanns, and L. Thiele. SPEA2: Improving the strength pareto evolutionary algorithm for multiobjec- tive optimization. In *Evol. Methods for Design, Optimisation and Control with Application to Industrial Problems*. 2002.
23. E. Zitzler and L. Thiele. Multiobjective optimization using evolutionary algorithms: A comparative study. In *Proc. Int'l Conf. on Parallel Problem Solving from Nature*, 1998.
24. E. Zitzler and L. Thiele. Multiobjective evolutionary algorithms: a comparative case study and the strength pareto approach. *IEEE Trans. Evol. Computat.*, 3(4), 1999.